

THE IMACS CLUSTER BUILDING SURVEY: V. FURTHER EVIDENCE FOR STARBURST RECYCLING FROM QUANTITATIVE GALAXY MORPHOLOGIES*

LOUIS E. ABRAMSON^{1,2,†}, ALAN DRESSLER³, MICHAEL D. GLADDERS^{1,2}, AUGUSTUS OEMLER, JR.³, BIANCA M. POGGIANTI⁴, ANDREW MONSON³, ERIC PERSSON³, AND BENEDETTA VULCANI^{4,5}

Submitted to The Astrophysical Journal

ABSTRACT

Using J - and K_s -band imaging obtained as part of the IMACS Cluster Building Survey (ICBS) we measure Sérsic indices for 2160 field and cluster galaxies at $0.31 < z < 0.54$. We compare the distributions for spectroscopically determined passive, continuously starforming, starburst, and poststarburst systems and show that previously established spatial/statistical connections between these types extend to their gross morphologies. Outside of cluster cores, we find close structural ties between starburst and continuously starforming, as well as poststarburst and passive types, *but not* between starbursts and poststarbursts. These results independently support two conclusions presented in a previous ICBS paper (Dressler et al.): 1) most starbursts are the product of a non-disruptive triggering mechanism that is insensitive to global environment, such as minor-mergers; 2) starbursts and poststarbursts largely represent transient phases in the lives of “normal” starforming and quiescent galaxies, respectively, originating from and returning to these systems in closed “recycling” loops. In this picture, spectroscopically identified poststarbursts constitute a minority of all recently terminated starbursts and the starburst phenomenon is largely decoupled from passive galaxy production in all but the densest environments.

Subject headings: galaxies: clusters — galaxies: evolution — galaxies: morphologies — galaxies: structure — galaxies: starburst — galaxies: poststarburst

1. INTRODUCTION

The quiescent galaxy population has grown since $z \sim 1$ in all environments (Butcher & Oemler 1978a; Faber et al. 2007; Moustakas et al. 2013). Commonly, new passive systems (hereafter PAS) are thought to descend from continuously starforming galaxies (CSF) wherein a “transformational event” depleted or removed cold gas supplies and prevented further star-formation (see Renzini 2006, §5 & references therein). Starbursts (SB) are oft-invoked catalysts for this metamorphosis (e.g., Dressler & Gunn 1983; Couch & Sharples 1987; Poggianti et al. 1999; Quintero et al. 2004; Hogg et al. 2006).

Key to the burst-driven evolutionary scenario is the ‘poststarburst’ (PSB; a.k.a. ‘E+A’ / ‘k+a’) galaxy population (Dressler & Gunn 1983; Zabludoff et al. 1996; Tran et al. 2004). These objects have spectra exhibiting deep Balmer absorption characteristic of short-lived A stars (signifying recent star-formation) but negligible emission (signifying little current star formation). Further, they may preferentially occupy a locus in color-

magnitude space between the ‘blue cloud’ of starforming systems and the passive-dominated red sequence (Yan et al. 2009; Mendel et al. 2012). Because these characteristics make poststarbursts compelling candidates for the CSF–PAS “missing-link”, starbursts emerge as important mechanisms enabling the former’s transformation into the latter. But how important are they?

In a previous paper from the IMACS Cluster Building Survey (ICBS; Dressler et al., 2013, hereafter Paper II) we asked: What fraction of passive galaxies descended through the CSF \rightarrow SB \rightarrow PSB \rightarrow PAS evolutionary channel? To address this, we first sought to determine if there were enough intermediate-redshift starbursts to account for the growth in the passive population between then and now. Surprisingly, we found far too many in all environments less dense than galaxy cluster cores (i.e., the isolated field, field and cluster-infalling groups, and the supercluster environment at $R_{cl} > 500$ kpc); assuming the starburst and poststarburst phases have similar lifetimes ($200 \lesssim \tau_{SB} \sim \tau_{PSB} \lesssim 500$ Myr; Poggianti et al. 1999; Oemler et al. 2009), and that all SBs ‘quench’ appropriately, the number of high-mass passive systems should have approximately doubled within a Gyr after $z \sim 0.4$, far outstripping observed growth (see e.g., van der Wel et al. 2007; Moustakas et al. 2013). Combined with our finding of a constant ratio of CSF- to SB-fractions across *all* environments, this discrepancy led us to conclude in Paper II that most starbursts do not move into the poststarburst population after a burst subsides. That is, most starbursts do not go on to exhibit a PSB spectrum and then transform into new passive galaxies. Instead, as suggested by Poggianti et al. (1999), we posited that SBs generally return to the “par-

* Data were obtained using the 6.5-m Magellan Telescopes at Las Campanas Observatory, Chile.

¹ Department of Astronomy & Astrophysics, University of Chicago, 5640 S Ellis Ave, Chicago, IL 60637

² Kavli Institute for Cosmological Physics, University of Chicago, 5640 S Ellis Ave, Chicago, IL 60637

³ The Observatories of the Carnegie Institution for Science, 813 Santa Barbara St, Pasadena, CA 91101

⁴ INAF-Osservatorio Astronomico di Padova, vicolo dell’Osservatorio 5, 35122 Padova, Italy

⁵ Kavli Institute for the Physics and Mathematics of the Universe, University of Tokyo, Kashiwa, 277-8582, Japan

[†] Corresponding author; labramson@uchicago.edu

TABLE 1
ICBS SPECTRAL TYPE STATISTICS & PROPERTIES

Type	Spec. ID	N_{tot}	N_{used}^a J/K_s	J -band SNR $25^{th}, 75^{th}$ pctl.	K_s -band SNR $25^{th}, 75^{th}$ pctl.
Passive	PAS	457	397 (87%) / 388 (85%)	63, 153	68, 130
Poststarburst	PSB	55	44 (80%) / 42 (76%)	42, 120	50, 119
Continuously starforming	CSF	1339	1077 (80%) / 1013 (76%)	35, 116	50, 115
Starburst	SB	304 ^b	213 (70%) / 191 (63%)	30, 92	43, 95

^a Galaxies with ≥ 75 (50) J (K_s) pixels above $1.5\sigma_{sky}$ with no r_e , b/a , or n fit flags.

^b 233 SBH + 71 SBO

ent” CSF class, remaining in a closed, CSF–SB–CSF recycling loop.

Finding starbursts to be inefficient quenching mechanisms, however, does not mean they are ineffective in terms of accounting for the increase in the passive fraction with time. To test this, we took the poststarbursts as proxies for those SBs which are quenching, or at least not participating in CSF–SB–CSF recycling.⁶ Yet still, PAS overproduction – now at earlier times – remained problematic: Given the frequency of $z \sim 1$ PSBs (see Lemaux et al. 2010), we expect the passive fraction at $z \sim 0.4$ also to be about twice what we observe. Combined with a similar constancy of the PAS:PSB ratio across all environments, this disagreement suggested that a closed, PAS–PSB–PAS recycling loop must also be active, running parallel to that of the starforming systems. In other words, many PSBs must descend from PASs, not the other way around.

Combining these findings, we constructed the following hypothesis: starforming and passive systems, respectively, typically remain in closed-loop cycles, with base levels of star-formation or general quiescence punctuated by brief periods of starburst activity. Absent external factors, SBs return to the parent class from which they came with those bursts *originating* in passive galaxies being briefly detectable as prototypical (spectroscopic) poststarbursts. Being unable to seriously alter the relative abundances of their parent types, SB/PSBs are thus not transitional stages in CSF \rightarrow PAS evolution, but transient phases in the lives of these “normal” systems.

Given the constancy of the ratio between parent- and burst-type fractions across a wide range of local densities, we proposed minor-mergers involving a gas-rich companion as the likely trigger for many intermediate-redshift starbursts (e.g., Mihos & Hernquist 1994; Kaviraj et al. 2009). Additional triggers – such as disk instabilities, tidal encounters, or accretion of cold gas from the inter-galactic medium – may be operational in the field or in the continuously starforming population. However, because they are expected to occur everywhere (Fakhouri & Ma 2009) and act on all galaxies regardless of host properties (Woods & Geller 2007), minor-mergers are the most compelling candidate for a general mechanism.

This scenario works well outside of cluster cores. In these special environments ($R_{cl} \lesssim 500$ kpc) however, the SB:PSB ratio is seen to approach unity and the PAS fraction rises substantially, removing the aforementioned

PAS overproduction problem. Thus, in agreement with many authors, we suggested that other processes dependent on a dense intra-cluster medium (ICM) – e.g., ram-pressure stripping (Gunn & Gott 1972) and starvation/strangulation (Larson et al. 1980; Bekki et al. 2002; Moran et al. 2007) – drive traditional CSF \rightarrow PAS evolution here, both by preventing SBs from returning to a CSF state and actively extinguishing star formation in CSF galaxies. Because gas disks in low-mass companions are not likely to survive the descent into these extreme environments, most PSBs in cluster cores likely *do* reflect the end-states of CSF-derived SBs instead of mergers onto PAS galaxies.

1.1. An Independent Test

The conclusions described above were based on spectroscopic and photometric data. However, there is a third avenue by which we can examine the role of starbursts in passive galaxy production: galaxy structure. In this paper, we probe the accuracy of our hypotheses from this independent perspective. By analyzing the Sérsic index distributions of the ICBS spectral types as derived from high-resolution near-infrared (NIR) imaging, we will show that the structural relationships between these systems not only support, but independently suggest, much of the picture we painted in Paper II.

We proceed as follows: Section 2 outlines the ICBS and the data used in this analysis; Section 3 describes our Sérsic index measurement routine; Section 4 presents our results. We provide a discussion in Section 5 and conclude in Section 6. Throughout, we take $H_0 = 72 \text{ km s}^{-1} \text{ Mpc}^{-1}$, $\Omega_m = 0.27$, and $\Omega_\Lambda = 0.73$. All magnitudes are quoted in the 2MASS system unless otherwise indicated.

2. DATA: THE IMACS CLUSTER BUILDING SURVEY

The ICBS is a spectrophotometric survey of four 27’-diameter fields containing five galaxy clusters at $z \sim 0.4$. Its objective is to characterize the evolution of *typical* galaxies across a range of environmental densities at an epoch in which cluster assembly is vigorously ongoing (Kauffmann 1995; De Lucia et al. 2004; McBride et al. 2009; Gao et al. 2012) and many transformational mechanisms are likely to be active.

Fields were drawn from the Sloan Digital Sky Survey (SDSS; York et al. 2000) and Red-Sequence Cluster Survey (Gladders & Yee 2005) using the cluster finding technique of Gladders & Yee (2000). Because of its relative insensitivity to relaxation state and our interest in cluster building, we opted for optical selection over gas-dependent techniques (e.g., X-ray selection) to avoid

⁶We adopt a similar poststarburst definition to that outlined in Poggianti et al. (1999, see §4), ensuring the majority of these systems are in fact post-burst and not post-truncation galaxies.

TABLE 2
ICBS ENVIRONMENTS

Env.	N_{tot}	J	N_{used}	K_s
Field + field groups	1164	892 (77%)	825 (71%)	
Supercluster ^a	471	387 (82%)	374 (79%)	
Cluster ^b	525	447 (85%)	435 (83%)	
Cluster core ^c	137	119 (87%)	114 (83%)	
TOTAL	2160 ^d	1731 (80%)	1634 (76%)	
TOTAL NON-CORE	2023	1612 (80%)	1520 (75%)	

^a Galaxies within ± 3000 km s⁻¹ of $\langle z \rangle_{cl}$ and $R_{cl}/R_{200} > 1.5$.

^b Galaxies within ± 3000 km s⁻¹ of $\langle z \rangle_{cl}$ and $R_{cl}/R_{200} \leq 1.5$.

^c Cluster galaxies with $R_{cl} < 500$ kpc.

^d Due to guide-star constraints, 3 objects from the ICBS catalogue were not imaged by FourStar.

sampling only well-virialized (i.e., built) systems. The latter are, in some sense, the most extreme environments in the universe, so processes occurring there may not reflect those driving the evolution of average galaxies – even those in clusters – at intermediate redshifts.

Details of the optical data comprising the bulk of the survey – obtained using the Inamori Magellan Areal Camera & Spectrograph (IMACS; Dressler et al. 2011) and Low Dispersion Survey Spectrograph III (LDSS3) on the Magellan-Baade & -Clay telescopes, respectively – can be found in Oemler et al. (2013a). However for convenience we review key aspects below.

2.1. Optical Spectroscopy

The ICBS is based on > 4800 spectra ($\lambda/\Delta\lambda \sim 600$) from 42 IMACS and 16 LDSS3 masks (3–4 hr exposures) obtained between 2004 and 2008. The wide field-of-view of IMACS permits simultaneous coverage out to $R_{cl} \lesssim 5$ co-moving Mpc, allowing relatively unbiased sampling of the entire (super-)cluster and projected field ecosystems.

The spectroscopic catalogue provides uniform, rest-frame spectral coverage from 3700–5200 Å for 2163 objects in the redshift interval $0.31 < z < 0.54$. These systems are roughly evenly split between five ‘metaclusters’ (see below; $N = 993$) and the projected, intervening field ($N = 1170$). Median signal-to-noise ratios (SNR) near 4500 Å range from 30 per 2 Å pixel at $r = 19$ to ~ 8 at $r = 22$ (SDSS system).

In Paper II these data were used to construct new galaxy spectral types and characterize field and cluster group-scale (sub-)structures. Below, we consider the four large-scale environments discussed in that paper: (1) the isolated field and field groups; (2) the supercluster and cluster-infalling groups ($R_{cl}/R_{200} > 1.5$); (3) the virialized cluster ($R_{cl}/R_{200} \leq 1.5$); and (4) the cluster core ($R_{cl} \leq 500$ kpc). We defer a discussion based on local density to a future paper.

In what follows, we also adopt the spectral type assignments from Paper II. However, to ease discussion, we combine starbursts identified by EW(H δ) (“SBH” in Paper II) with those identified by EW([OII] $\lambda 3727$) (“SBO”) into single starburst class (“SB”, herein). The reader should note first that these systems are not necessarily ULIRG-like objects, but galaxies whose star-formation rates (SFR) are enhanced by factors of $\sim 3 - 10$ over the past (few Gyr) average. Again, we are interested in studying processes affecting typical

intermediate-redshift galaxies and therefore characterizing the role average (i.e., moderate) starbursts play in galaxy evolution. Also of note, the SBH class likely contains objects both at and decaying away from their peak period of star formation (see Dressler et al. 2009, and Paper II, §§2.2 & 4.6 for a more detailed discussion). Our results are qualitatively unchanged if either SB class is examined independently.

Tables 1 & 2 present the relevant spectral and environmental definitions and statistics.

2.2. NIR Imaging

Structural parameters are derived from J - & K_s -band images of the four ICBS fields acquired in Nov. 2011 and Feb. 2012 using the FourStar camera on Magellan-Baade (Persson et al. 2008, 2013 in preparation). At the redshifts considered here, these bands probe the light (dominated by G–K giants) from established stellar populations and are largely insensitive to gas and dust, thus providing almost direct access to the underlying galactic structure which we seek to characterize. These data and their reduction will be described in detail in a future paper, but we list here properties relevant to the current analysis.

Each IMACS field was tiled with FourStar in a 3×3 mosaic. Final images (~ 0.25 deg²) were constructed using A. Monson’s pipeline, which employs SExtractor, SCAMP & SWARP (Bertin & Arnouts 1996; Bertin 2010a,b), and IRAF IMCOMBINE to astrometer, zeropoint-normalize, distortion-correct, and co-add all pointings across a mosaic. Astrometric and distortion solutions were computed jointly for J - & K_s -band images, minimizing filter-dependent systematics which could bias morphological measurements.

Typical limiting depths for these images are $J = 23.3$ and $K_s = 21.4$ (5σ point-source, $1''0$ aperture). At magnitudes of $J = 21.0$ and $K_s = 18.5$, encompassing 90%–95% of the spectroscopic targets, these data yield median SNRs for point sources of 35 and 51 in J and K_s , respectively.

Seeing conditions ranged from $0''.5 - 1''.0$ in J - and $0''.3 - 0''.9$ in K_s -band with median values around $0''.55$ in both.

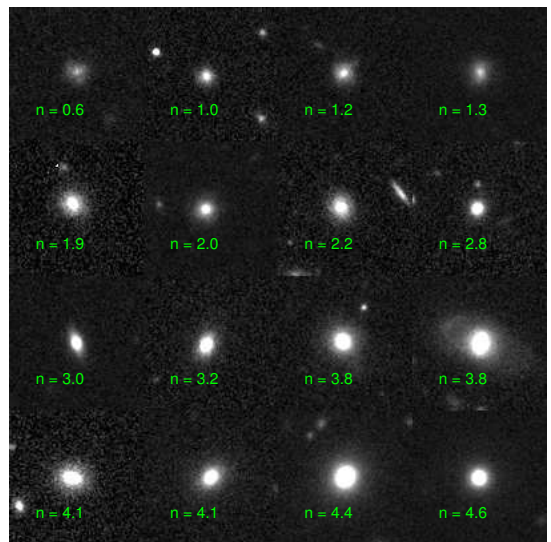


FIG. 1.— J -band source thumbnails arrayed by increasing Sérsic index. Image stamp-sizes are $16''$ and all are scaled uniformly.

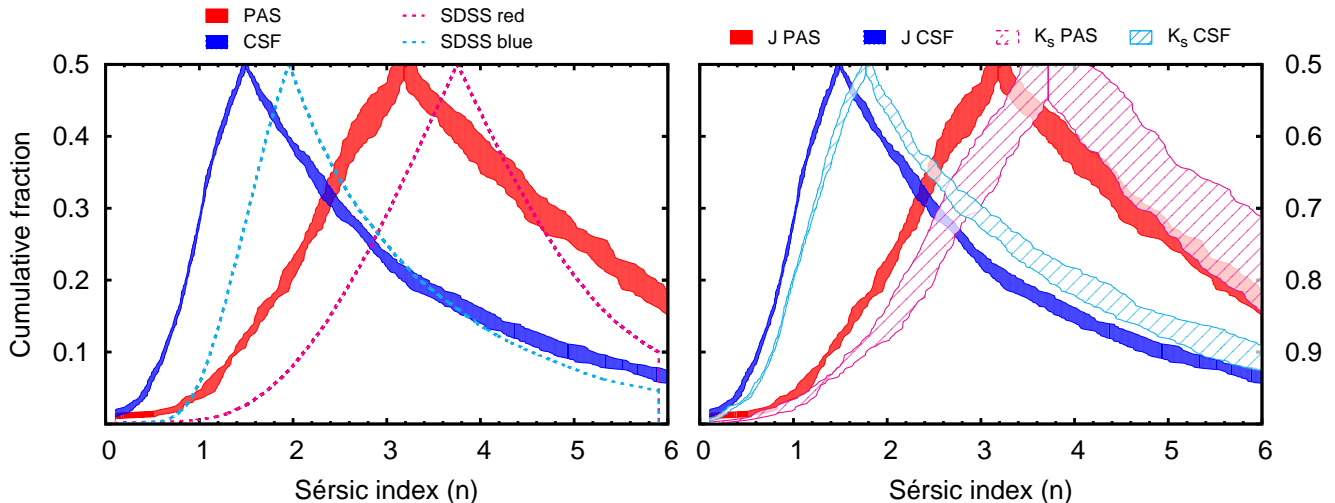


FIG. 2.— *Left panel:* Magenta and cyan dashed-lines are, respectively, the folded, cumulative, z -band Sérsic index distributions (see text Section 4) for $\sim 29,300$ red and $\sim 14,400$ blue galaxies from the SDSS. Objects are drawn from the group catalogue of Yang et al. (2007) with measurements from the NYU VAGC (Blanton et al. 2005). Red and blue shaded areas are the J -band distributions for ~ 400 PAS and ~ 1100 CSF galaxies from the ICBS, respectively. Thickness represents the minimum/maximum values obtained at a given n over six fitting runs. *Right panel:* A comparison of our J - (solid) and K_s -band results (striped areas). Combined with Fig. 1, the consistency of these results give us confidence our measurements are (at least statistically) sufficiently robust for the current purposes.

As FourStar pixels are $0''.16$, the point-spread-function (PSF) is well-sampled in all but one image, where it is mildly under-sampled. As our final results are robust to PSF selection (see below), the following analysis was not modified for this field.

2.3. A Note on Incompleteness

As discussed in Paper II, the ICBS spectroscopic sample covers approximately 50% of the photometric catalogue down to $r \approx 22.5$. As it is unbiased with respect to spectral type at the 90–95% level, no differential incompleteness corrections were implemented in the following analyses. Significant corrections are necessary if one wishes to discuss mass-dependent phenomena (such as evolution between spectral types) using the magnitude-limited ICBS sample. However, because we will largely concern ourselves with characterizing the spectral types individually, we do not apply any mass-incompleteness corrections below. Instead, we repeat our analyses using a mass-complete sample ($M_{\text{stellar}} \geq 2.5 \times 10^{10} M_{\odot}$) and refer to this when directly comparing galaxy counts across spectral types.

3. STRUCTURAL PARAMETER ESTIMATION

Sérsic indexes were measured by fitting single Sérsic profiles using GALFIT v3.0.4 (Peng et al. 2002, 2007), with SExtractor v2.8.6 employed for source detection and ancillary image production. Software has been developed for automated, batch-mode operation of GALFIT – notably GALAPAGOS (Barden et al. 2012) – but flexibility is often sacrificed for speed. Because our analysis required a spatially variable PSF, and the ability to add model components/parameters was considered useful,⁷ we created our own fitting routine.

For each spectroscopic source, a 200×200 kpc stamp was cut from the full, background-subtracted FourStar

⁷ICBS ground-based imaging spans $grizJK_s$. Though not implemented here, future analyses of the full photometric data set may draw upon these additional capabilities.

mosaic and the local gain/exposure time calculated from a coverage map. A local PSF was then either constructed from an inverse-variance weighted stack of the nearest 10 stars or selected from a library of models. The latter were created from multi-component Sérsic fits to candidate PSF stars and visually inspected to ensure quality. Below, we discuss results from five runs using this implementation (taking the five nearest PSF models) and one run using the composite, empirical PSF. In the interest of clarity, all sample statistics are quoted from the “principal” run using the nearest model PSF.

After PSF selection, SExtractor produced basic positional, geometric, and photometric data for GALFIT input. The source nearest to the spectroscopic catalogue location was defined as the ICBS target (“primary”), but all primaries having no pixel within $1''.0$ of this fiducial position – derived from histograms of ICBS-SExtractor centroid offsets – were flagged for possible confusion and excluded from later analysis. These tended to occur where the ICBS source was of low-to-no NIR significance (i.e., rest-frame $B - V \lesssim 0.5$) and resulted in the loss of 57 (136) objects in J (K_s).

On-stamp stars were PSF-subtracted before galaxy fitting. Galaxies with $m - m_p < 2.0$ and $|\overline{r} - \overline{r}_p| \leq 25$ kpc – where $m_{(p)}$, $\overline{r}_{(p)}$ are magnitudes and transverse positions of (primary) sources – were fit jointly with the primary. Pixels outside an ellipse $3.0 \times \text{KRON_RADIUS}$ from these “fit-worthy” galaxies were masked along with non fit-worthy sources and star-subtraction cores.

GALFIT was allowed to determine a constant background level for each stamp. Fixing the sky to zero or a value based on non-source pixel statistics does not affect our results, though it can significantly affect fits for individual sources (see Section 4).

“Successful” fits were those whose output parameters (half-light radius, r_e ; axis ratio, b/a ; and Sérsic index, n) converged away from fitting constraints and were not flagged as unreliable by GALFIT. The first condition essentially imposed a minimum-size criterion which,

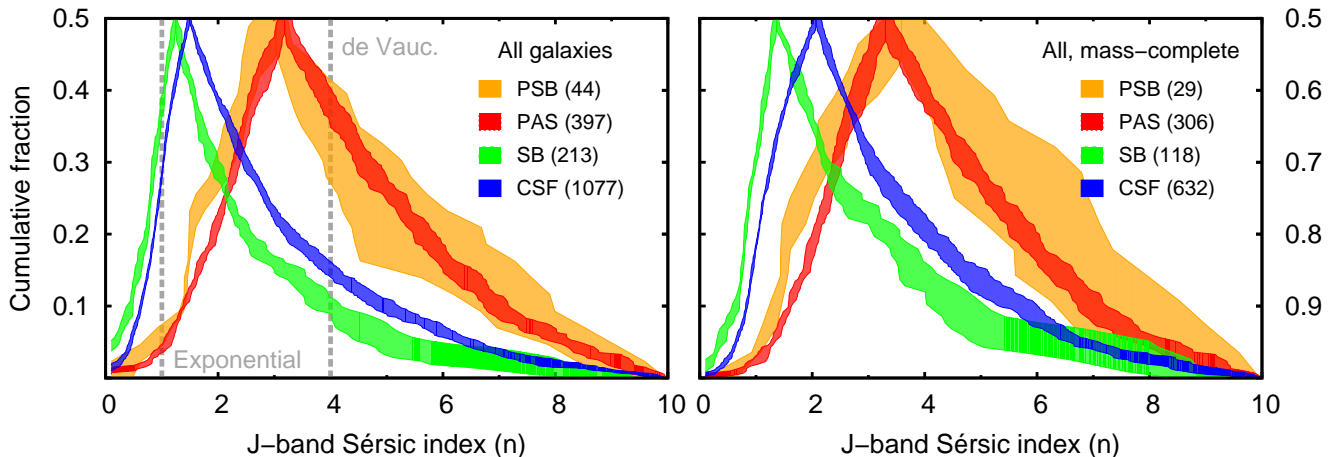


FIG. 3.— *Left panel:* J -band Sérsic index distributions for all ICBS galaxies. Quantities in parentheses give N_{gals} in the principal distribution of each type (see Section 3). Good agreement between PSB (orange) and PAS (red), as well as SB (green) and CSF (blue) distributions is apparent, as is a significant discrepancy between the SB and PSB bands. The former systems tend (in the median) towards the exponential profiles of local spirals, the latter towards the de Vaucouleurs profiles of giant ellipticals. *Right panel:* Distributions for galaxies with stellar masses $M \geq 2.5 \times 10^{10} M_{\odot}$, where the ICBS is largely complete for all spectral types. As these are essentially identical to the magnitude-limited results, we do not believe mass-incompleteness is a significant source of bias in our analysis. Alternately put, the spectral-type structural relationships do not appear to be a strong function of stellar mass.

through experimentation, was found to be ~ 75 pixels (J) or ~ 50 pixels (K_s) detected at $\geq 1.5\sigma$ above sky RMS. We apply this (somewhat arbitrary) cut, roughly limiting the sample to $\text{SNR} \gtrsim 20$, but note that adjusting it either way has a negligible effect on our results.

After excluding mis-identified, poorly fit, and small sources, the final sample contains 1731 (1634) galaxies in J (K_s) suitable for analysis. As shown in Table 1, the failure rate is unbiased with respect to spectral type at the $\sim 10\%$ level in J (which we will use for the majority of our analyses) so we do not correct for differential failure rate in what follows.

4. RESULTS

The model presented in Paper II suggests starbursts and poststarbursts should physically resemble CSF and PAS galaxies, respectively, but not each other. This is a statement about galaxy morphology and structure. Ideally, we would test our model in terms of the former as fine-grained details (e.g., the presence of spiral arms or tidal features) place the strongest constraints on formation / transformation mechanisms. However, for sources at $z \sim 0.4$, true morphologies can be assessed only from space-based imaging and covering the ICBS with the *Hubble Space Telescope* (*HST*) would require ~ 1000 pointings. Fortunately, high-quality ground-based data (such as we have obtained) is more than adequate to allow characterizations of the basic structural properties of our systems. Since determining even the average diskiness or bulginess of the spectral types would provide a strong test of our hypotheses, we pursue this avenue here. As is common, we parameterize galactic structure using the Sérsic index, n (Sérsic 1968).

4.1. Fitting Accuracy

Measuring Sérsic indices to high accuracy is difficult (e.g., Häussler et al. 2007; Hoyos et al. 2011; Yoon et al. 2011). For example, across our six runs, uncertainties

in individual fits due to background estimation and PSF selection alone range from $\sim 5\%$ at $n = 1$ to $\sim 30\%$ at $n = 4.0$ – 4.5 , irrespective of spectral type. Yet, because we are interested in the relationships between classes of galaxies – and therefore index *distributions* – we avoid many of the complexities associated with this endeavor. For our purposes, measured differences will be quantitatively meaningful provided the fits (though uncertain) are unbiased; i.e., provided the spectral types span comparable SNR ranges. As this is the case (see Table 1), relative comparisons between distributions are reliable.

That said, we believe our measurements are reasonably accurate in an absolute sense. Though we have not tested our routine on simulated sources, we can assess our fitting accuracy both qualitatively and quantitatively in several ways.

Qualitatively, our measured Sérsic indices correlate well with visual impressions. Figure 1 shows J -band cut-outs for some of our higher-SNR sources. As n increases, systems clearly progress from disk- to bulge-dominated. Comparisons of ICBS Sérsic index histograms (not shown) also appear consistent with V -band results from the low-redshift, Wide-field Nearby Galaxy Cluster Survey (WINGS; Fasano et al. 2012, see their Fig. 18). From these, we find our PASs to be consistent with a mixed S0/E population and our CSFs to be similar to local spirals, as expected.

Quantitative assessments are provided in Figure 2. In the left panel, we compare z -band fits from the NYU Value-Added Galaxy Catalog (VAGC; Blanton et al. 2005) for photometrically selected red and blue SDSS galaxies to J measurements (roughly rest-frame z) of our PAS and CSF systems. To approximate the mean ICBS environment, the comparison sources ($z \leq 0.1$) were drawn from the group catalogue of Yang et al. (2007). In this and all similar plots below, we show *folded* cumulative distributions, i.e., cumulative distributions reflected at their medians. This (somewhat non-traditional) for-

TABLE 3
SÉRSIC INDEX DISTRIBUTION STATISTICS, NON-CORE GALAXIES

Type	$\mathcal{L}(\epsilon \text{ PAS})^a$ (dex)		Median (n)		IQR (n) ^b		$f(n < 2)^c$	
	J	K_s	J	K_s	J	K_s	J	K_s
PAS	3.1 ± 0.1	3.7 ± 0.3	2.9 ± 0.2	3.1 ± 0.4	0.23 ± 0.02	0.15 ± 0.02
PSB	4.1 ± 0.6	2.9 ± 0.5	3.2 ± 0.2	3.4 ± 0.3	3.4 ± 1.0	3.2 ± 0.3	0.26 ± 0.03	0.27 ± 0.01
CSF	1.5 ± 0.1	1.7 ± 0.1	1.9 ± 0.1	2.2 ± 0.1	0.62 ± 0.01	0.56 ± 0.01
SB	-25 ± 1	-26 ± 1	1.3 ± 0.1	1.6 ± 0.1	1.4 ± 0.1	1.7 ± 0.1	0.70 ± 0.01	0.64 ± 0.01

^a Logarithmic likelihood that a distribution is drawn from the PAS over the CSF parent. Positive values denote sample is more likely to have come from the PAS class.

^b inter-quartile range; 75^{th} minus 25^{th} percentile.

^c Fraction of galaxies with $n < 2$.

mat gives a good sense of a distribution’s width and skew – as a histogram would – but has the advantage of avoiding binning. A complication is that ordinates are reversed at every median. Hence, the reader must use the left-hand axis to interpret the rising part of each band, but the right-hand axis to interpret the falling part.

There is a systematic shift of $\Delta n \approx -0.5$ and slightly longer high- n tails in the ICBS distributions, but the global similarity of these to the SDSS/VAGC results is apparent. Given the possible influence of redshift evolution, color versus spectroscopic selection, differences in fitting methods, source resolutions,⁸ and sample size in addition to any real fitting errors, the correspondence between these results suggests that our measurements are sufficiently reliable for the current analysis. Ultimately, the most relevant aspect to note is the near-identical separation between red/blue distributions in either sample, implying both analyses have comparable power to discriminate between disks and spheroids.

A final test we perform is an internal cross-check of our J - and K_s -band results. This is plotted in the right-hand panel of Fig. 2. Reassuringly, these agree well. The small systematic offset between the two measurements could, again, be due to many factors besides fitting error. Some of the shift may be physically meaningful (a factor of two in wavelength separates the bandpasses), but the loss of low surface-brightness features (e.g., disks) due to the higher sky backgrounds in K_s surely also plays a role. Regardless, because the offset is essentially uniform, errors contributing to it should not be biasing our results, allowing meaningful comparisons of results obtained independently in either band. (Indeed, as shown in Table 3, our main results hold across both.) This being the case, since a higher fitting success rate was achieved in J , we discuss these results below unless otherwise indicated.

4.2. Spectral-type Distributions

The left panel of Figure 3 presents our first main result: the full Sérsic index distributions for all reliably fit ICBS galaxies. Distribution widths correspond to the minimum/maximum values obtained at a given n over the six fitting runs discussed in Section 3. We introduce our analytical processes and comparison metrics here before testing the effects global environment and mass completeness have on this result.

⁸ $\text{FWHM}_{\text{SDSS}} \approx 1''2 = 1.4$ kpc at $z = 0.06$, while $\text{FWHM}_{\text{ICBS}} \approx 0''5 = 2.7$ kpc at $z = 0.40$. Alternately, at those redshifts, 1 kpc spans 2.2 SDSS pixels, but only 1.2 FourStar pixels. Both types of “resolution” affect the accuracy of GALFIT.

The two most obvious characteristics of this plot are also the most important. First, the SB–CSF and PSB–PAS distributions, respectively, display unambiguous similarities. Second, there is an equally clear disparity between the SB and PSB distributions; the former is shifted to values characteristic of disks ($n \sim 1$) while the latter is shifted to those characteristic of bulge-dominated systems ($n \sim 3 - 4$). Although the dissimilarity of the PAS and CSF distributions link these conclusions, there is no *a priori* astrophysical reason to expect starbursts to resemble their supposed antecedents (CSFs) but not descendants (PSBs). We will see later that these statements constrain different parts of the recycling model outlined in Section 1.

These (dis-)connections can be quantified in several ways. Comparing the medians, inter-quartile ranges (IQR), and fractions of galaxies with $n < 2$, $f(n < 2)$ – a generic upper-limit for “diskiness” (Fisher & Drory 2008) – confirms visual impressions. First, the non-starforming types display identical medians ($n \simeq 3.1$) and distribution widths (IQR $\simeq 3.0$), within the scatter of the fitting runs ($\sigma_{\text{median}} \approx 0.2$; $\sigma_{\text{IQR}} \approx 0.7$). The distributions for the starforming types, though not as consistent, remain quantitatively very similar. Both have median $n \sim 1.0 - 1.5$ and $f(n < 2) > 60\%$, suggesting that most of these systems are classic exponential disks. This is to be contrasted with the poststarbursts, which have $f(n < 2) \sim 25\%$.

For a final quantitative comparison, we calculate the relative likelihood, $\mathcal{L}(\text{child} \in \text{PAS})$, that the “child” SB or PSB distribution were drawn from the PAS over the CSF parent:

$$\mathcal{L}(\text{child} \in \text{PAS}) \equiv \log \left(\frac{P_{\text{child,PAS}}}{P_{\text{child,CSF}}} \right), \quad (1)$$

where P is the usual probability metric from a two-sided Kolmogorov-Smirnov (KS) test. This approach uses all the information in the distributions, avoiding binning and parameterization. Across our six runs in J , we find $\mathcal{L}(\text{PSB} \in \text{PAS}) \geq 4.0$ while $\mathcal{L}(\text{SB} \in \text{PAS}) < -26$. In other words, the PSBs have a high likelihood of having come from the PASs (over CSFs) while there is essentially zero probability the SBs were drawn from that parent. Indeed, the raw probability $P_{\text{KS}}(\text{PSB} \in \text{PAS}) \geq 0.38$ for all trials, consistent with the full PSB distribution being drawn from the passive distribution. Given the limitations of the KS test, however, we do not weigh this fact too heavily.⁹ Regardless, the lack of similarity between

⁹For example, the raw probabilities do not directly link SBs to

starbursts and poststarbursts is clear and real, as is the close structural relationship between the starforming and quiescent types, respectively.

4.3. Mass Incompleteness

So far we have examined the full magnitude-limited ICBS sample ($r \lesssim 22.5$). Because it gives maximal statistical leverage this is the best sample to use to characterize the spectral types individually. However, since the types span different mass ranges, it may be inappropriate to use when cross-comparing their structural distributions. To determine if the magnitude-limited results are biased, we reanalyze a sub-sample containing only galaxies with $M_{\text{stellar}} \geq 2.5 \times 10^{10} M_{\odot}$ (Salpeter IMF; see Oemler et al. 2013a), corresponding to the $\sim 80\%$ ICBS completeness limit. The results are plotted in the right-hand panel of Figure 3. Clearly, the global trends from the full sample remain largely unchanged; using our log-likelihood statistic, we find $\mathcal{L}(\text{PSB} \in \text{PAS}) = 1.6 \pm 0.7$ for the PSBs (with $P_{KS}(\text{PSB} \in \text{PAS}) > 0.4$ for five of the six runs), but $\mathcal{L}(\text{SB} \in \text{PAS}) < -13$. (Note that some of the likelihood change is driven by the reduction in sample size.) Although the mass-limited CSFs appear slightly bulgier – perhaps reflecting the correlation of bulginess with mass (Benson et al. 2007; van der Wel 2008; Bell et al. 2012) – the SBs are still clearly structurally related to these systems and equally clearly distinct from the PSBs.

As mass incompleteness does not appear to be a significant source of bias in our analysis, we will continue to use the magnitude-limited sample, below.

4.4. Environmental Dependence

All results above were derived using a combination of cluster (core + non-core), supercluster, and field galaxies. Findings from Paper II suggest such mixing is not inappropriate: the fractional relationships between the spectral types point to recycling being active (if not dominant) everywhere outside of cluster cores. However, we can also test this assumption using the structural data. We begin by plotting separately the Sérsic index distributions for the field, supercluster, and cluster sub-samples in Figure 4.

In the field (top panel) the picture is identical to the combined result; we find $\mathcal{L}(\text{PSB} \in \text{PAS}) = 3.3 \pm 0.6$ for poststarbursts, but $\mathcal{L}(\text{SB} \in \text{PAS}) < -12$ for starbursts. In fact, if anything, the here picture is even more clear: PSBs and SBs have $\langle P_{KS} \rangle \sim 0.5$ of belonging to the PAS or CSF parent, respectively, with no run having $P_{KS} < 0.2$.

In the supercluster (middle panel), though likelihoods drop significantly (due, in part, to the smaller number of systems), the same general trends emerge for the starbursts as seen in the field. These systems exhibit $\mathcal{L}(\text{SB} \in \text{PAS}) < -6$, their distribution reflecting the shape of the CSFs to high fidelity although the latter have moved to slightly higher n overall. The lack of poststarburst systems prohibits us from constraining their relationship to the PASs, but we note that the two well-fit PSBs in this environment have Sérsic indices that fall precisely at the median value of the PAS distribution ($n \approx 3$).

CSFs, but we will argue in later that this is the only physically acceptable interpretation for most of these systems.

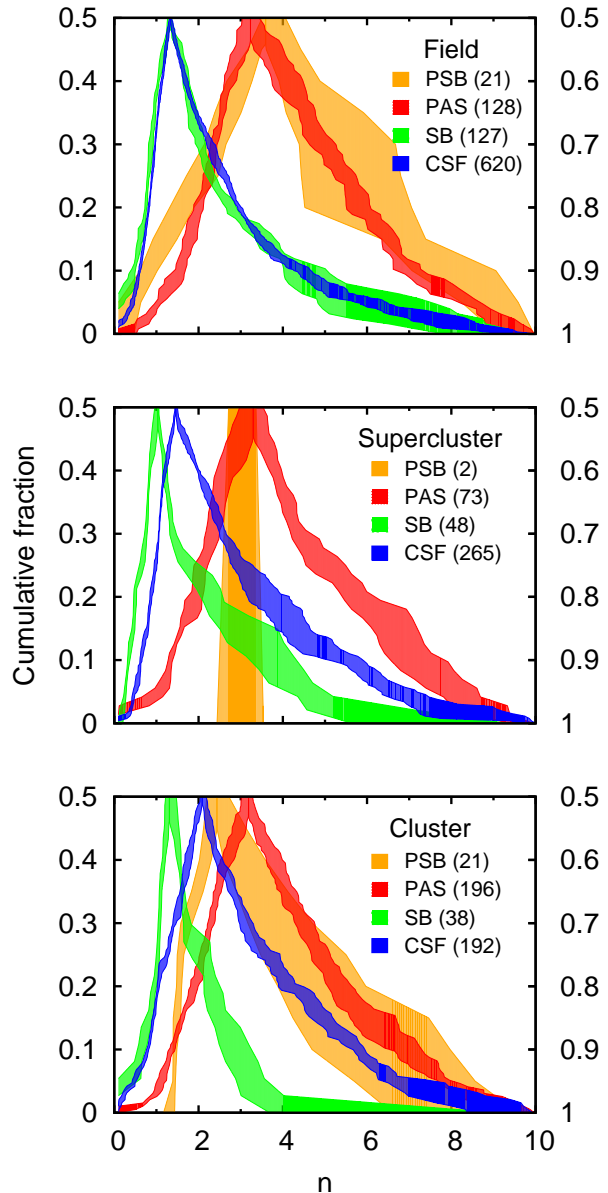


FIG. 4.— Sérsic distributions for three of the ICBS large-scale environments. *From top:* Field (isolated galaxies and groups); supercluster (infalling galaxies and groups); virialized cluster and cluster core. In the field, the burst classes are statistically indistinguishable from their respective non-burst “parents”. In the supercluster, though we have little power to constrain the poststarbursts, the active bursts retain strong similarities to the CSF types. In the cluster, both burst-types diverge from the non-bursts; PSBs here are diskier than their field counterparts, resembling the CSFs as closely as they do the PASs. These shifts suggest additional mechanisms may be at work in these dense environments.

However, in the cluster proper (bottom panel) the picture changes. First, it is clear that CSFs in this environment are considerably more bulge-dominated than those in the field. Their subtle departure from the starbursts in the supercluster is also exacerbated. This displacement may simply be a manifestation of the well-known morphology–density relation (Dressler 1980; Dressler et al. 1997; Postman et al. 2005) though interestingly it is not seen in the PAS population. Con-

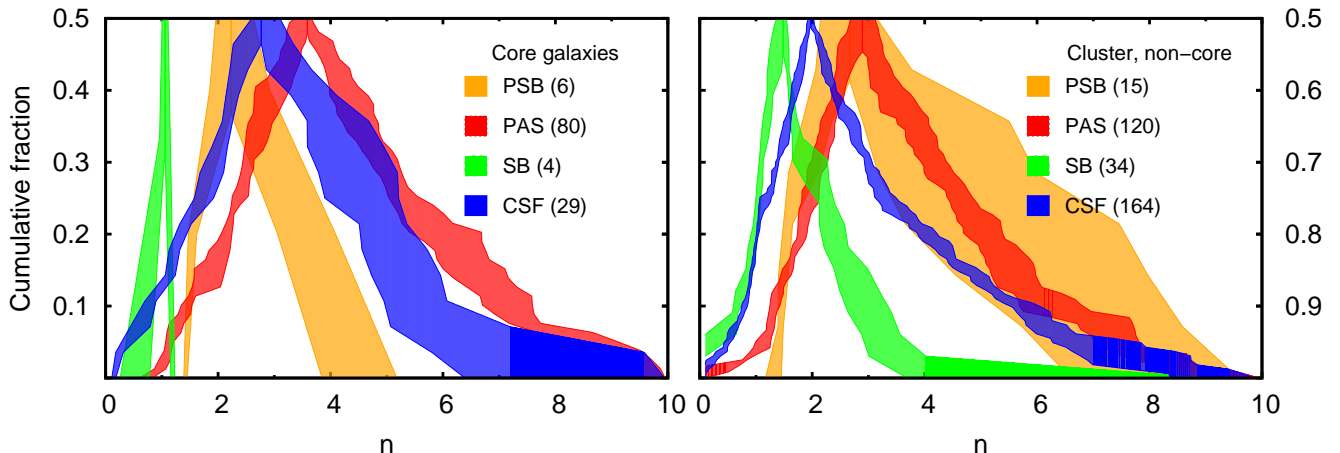


FIG. 5.— *Left*: J -band Sérsic index distributions for cluster core galaxies ($R_{cl} \leq 500$ kpc). While the active starbursts in cluster cores are still diskier, the parent–daughter relationships between the burst and non-burst classes in this environment are substantially degraded. Notably, the post-starbursts in the core have Sérsic indices between those of the SBs and PASs (or, alternately, close to those of the CSFs). These facts suggest mechanisms unique to dense environments (e.g., as ram-pressure stripping or starvation) may be causing a “leak” from CSF to PAS populations through active quenching or starburst-driven evolution. Population fractions from Paper II also suggest the latter is occurring, here. Note that, when this population of objects is removed (*right panel*), the relationship of cluster PSBs to the PASs is strengthened compared to the full cluster sample shown in the bottom panel of Fig. 4.

versely, cluster PSBs appear to be diskier than their field counterparts, moving closer to the starforming systems. This shift is reflected by the KS statistics: with $0.1 < \mathcal{L}(\text{PSB} \in \text{PAS}) < 1.1$, PSBs appear only marginally more likely to have come from the PASs over the CSFs.

Yet, PAS–PSB–PAS recycling may still be active in the cluster environment. If the dense ICM of the cluster *core* is providing additional processing as we expect, core galaxies may be biasing a significant trend here that would otherwise be similar to those of the field and supercluster.

To test this, in Figure 5 we plot the distributions for a “core-only” sample (left-hand panel) and the cluster with those galaxies removed (right-hand panel). Although statistics are limited, much of the shift to diskier PSBs indeed appears to be driven by those systems in the innermost 500 kpc of the cluster (modulo projection effects), where ram-pressure or tidal stripping may be playing large roles. Comparing the core-excised sample to the full cluster sample (Fig. 4, bottom) reveals the gap at low- n between the PSBs and PASs to have largely disappeared. Though, to the eye, there may still be some ambiguity between the non-core PSBs and CSFs at low- n , the KS metric reveals the former now to be 63 times more likely to have come from the PASs on average, up from ~ 3 in the full cluster sample. (The raw KS probability $P_{KS}(\text{PSB} \in \text{PAS})$ is also always > 0.2 , while in four of the six runs $P_{KS}(\text{PSB} \in \text{CSF})$ is less than 1 percent.)

These likelihoods represent conservative bounds to the true probabilities because the core-excised sample almost certainly includes “overshoot”/“backsplash” galaxies (Balogh et al. 2000; Moore et al. 2004; Bahe et al. 2012), i.e., systems which have been processed by the core but now lie at larger radii.

Given the trend of KS results, it seems that the *unprocessed* cluster population likely exhibits the same structural connections as those in the field and supercluster environments. If so, this would imply – as suggested in

Paper II – that there are only two significant environments in terms of the relationships between the spectral types: the highest-density regions of the universe, and everywhere else. If those galaxies living “everywhere else” (i.e., the overwhelming majority of systems) are examined, one obtains the distributions plotted in Figure 6. Here, the spectral type relationships are entirely unambiguous. Statistics – medians, inter-quartile ranges, $n < 2$ fractions, and $\mathcal{L}(\text{child} \in \text{PAS})$ values – describing these “non-core” distributions are presented in Table 3. Unless otherwise specified, the discussion in the next section will refer to this sample.

We have examined the distributions for a “group-only” sample comprised of galaxies identified in Paper II to be in field and cluster-infalling groups of ≥ 6 spectroscopic members. These results are entirely consistent with those of the field / supercluster.

5. DISCUSSION

As shown in the previous section, the structural connections between the spectral types are the same as those exhibited by their population fractions: the SB and CSF as well as PSB and PAS types resemble each other closely, but the active- and post-starbursts are highly dissimilar. However, while necessary, showing that starbursts are disk-dominated and poststarbursts are bulge-dominated is not sufficient to demonstrate that the closed recycling loops we posited are in fact operational. Indeed, many others – using both 1D and 2D fitting techniques – have found low-redshift poststarbursts to be comparably bulge-dominated to passive systems (see e.g., Quintero et al. 2004; Balogh et al. 2005; Yang et al. 2008; Mendel et al. 2012; Bell et al. 2012) but used this to support the traditional CSF \rightarrow SB \rightarrow PSB \rightarrow PAS quenching scenario we believe to be sub-dominant. Our goal here is to determine if these structural relationships are consistent with (or indeed independently suggestive of) the recycling scenario we presented in Paper II.

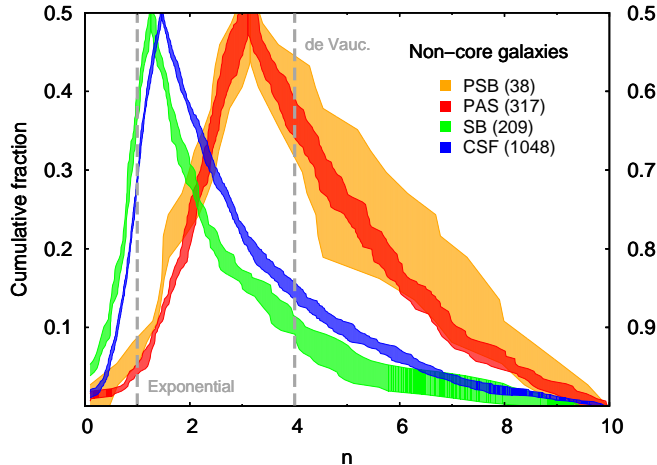


FIG. 6.— Final Sérsic distributions for all galaxies residing outside of cluster cores. Properties are listed in Table 3.

We turn first to the starforming systems. It is clear that the starbursts are, in general, the diskier galaxies in all environments. This fact is key: it implies that whatever is triggering the majority of bursts must be gentle. Whether they actively destroy disks or merely build bulges, violent interactions would wash-out the strong clustering around $n = 1$ displayed by these systems. That this is not the case suggests most SBs cannot evolve into the bulge-dominated PSBs; they are not undergoing the necessary structural transformation. It would seem, therefore, that these systems *have no choice* but to return to the CSF population after their current episode of enhanced star-formation subsides. (This is true even if, in some environments, the latter class is slightly “bulgier” than the SBs, on average.) Thus, the starforming recycling loop we proposed earlier emerges naturally from the structural data as well.

But what of the quiescent systems? As mentioned in Section 1, because SBs so outnumber PSBs, showing that most CSF-derived SBs do not evolve into PSBs does not imply that most PSBs do not descend from CSF-derived SBs. To test the second statement, we again take the PSBs as proxies for all starbursts not involved in CSF–SB–CSF recycling. The bulginess of these systems then suggests one of two things: (1) PSBs represent the subset of CSF-derived starbursts which *have* undergone major transformational events (i.e., major-mergers) and are now quenching; (2) PSBs originate in systems which are bulge-dominated *ab initio*.

Unfortunately, the structural similarity between the PSB–PAS classes is not, by itself, enough to clarify this ambiguity. As they are bulge-dominated, pressure-support is significant in the non-starforming systems. Therefore, we would not expect the signature of any transformational mechanism to be easily detectable. Hence, given only a strong “family resemblance” we cannot immediately differentiate between the two cases outlined above. However, we can make progress by attacking the problem from the opposite end, asking: Are there sufficient SBs involved in major-mergers to account for the PSB population? If so, PSB \rightarrow PAS evolution could readily explain the structural trends. If not, our recycling scenario would be favored.

To address this question, we performed a visual inspec-

tion of the J -band data, looking for galaxies which displayed clear signs of interactions with similar-sized systems without reference to their spectral type.¹⁰ Each object was graded from 100×100 kpc cut-outs on a scale of 0 to 2 (0 = no evidence of merging, 2 = definite merger in progress) with a subset of the objects graded twice after a random rotation and/or reflection. Of these objects, about 10% moved from grade 1 (possible merger; close companion or tidal feature) to grade 2 (obvious disruption from neighbor, large tidal tails, or “train-wreck” appearance) upon second viewing, so we include as “confirmed” major-mergers all grade 2 systems plus an additional 10% of the number of grade 1 systems.

In our combined, mass-limited, non-core sample (drawn from the full ICBS catalogue, not the subset of successfully fit galaxies), we find $\sim 3\%$ (PASs) to $\sim 6\%$ (SBs) to be involved in major-mergers. This result agrees well with that of Bell et al. (2006), who find $5\% \pm 1\%$ of all galaxies at $0.4 < z < 0.8$ to be merging using the same stellar-mass limit we apply ($M \geq 2.5 \times 10^{10} M_{\odot}$). We are also in agreement with Williams et al. (2011), who find a $6\% \pm 1\%$ merger fraction for galaxies at $0.4 < z < 2.0$ with $M \geq 3.2 \times 10^{10} M_{\odot}$. For the SB class, this fraction corresponds to 11 systems.¹¹ As there are 26 PSBs in the sample, taken at face value the number of major-merging active starbursts would seem to be able to account for slightly more than a third – but not most – of the poststarbursts, implying the recycling scenario must be active (if not dominant) as we suggest in Paper II.

We acknowledge, however, that this is a highly uncertain estimate. Two major factors drive this uncertainty: merger identification and remnant properties. We now try to constrain the effects each of these could have on our conclusion.

Regarding the issue of identification, there are two concerns: (1) merger features (e.g., tidal tails) may not be obvious at all merger stages; (2) mergers might occur on timescales much shorter than those over which spectral indicators change. If either is the case, we would have underestimated the true number of merging starbursts.

With respect to the latter concern, while the range of theoretical values for major-merger visibility timescales is large – radial separations / morphological disturbances depend on the myriad configurations and properties of the galaxies involved – it seems safe to say that $\sim 0.5 - 2.0$ Gyr are reliable bounds (e.g., Lotz et al. 2008; Conselice 2009; Lotz et al. 2010a,b). Considering our data span approximately 2 Gyr and SB indicators are sensitive to timescales ≥ 200 Myr, neither our data set nor spectral categorization should significantly under-sample the merger rate. That is, our data provide a sufficiently long baseline to capture most of a merger and our spectral definitions respond quickly enough to ensure that most merging starbursts fall in the SB class.

Misidentification of merging systems as non-mergers – because, for example, the galaxies are at large sepa-

¹⁰Results from *HST* data are inconclusive. Cluster surveys (e.g., Dressler et al. 1999; Tran et al. 2003; Poggianti et al. 2009) find PSBs to be generally pristine late- or early-type disks. Field studies (e.g., Tran et al. 2004; Yang et al. 2008) find many to display morphological irregularities indicative of recent mergers.

¹¹The mass-limit for this class is extended down to $M_{\text{stellar}} \geq 1.7 \times 10^{10} M_{\odot}$ to account for up-scattering of 1:3 mergers into the full mass-complete sample.

rations, have just coalesced, or do not display disturbed morphologies – is more problematic. Turning to Figs. 4 & 11 of Lotz et al. (2008) and examining their “Sbc” model (slightly more massive than our average SB but consistent with its diskiness) we find that, while (projected) pair separations of > 50 kpc are expected to last for perhaps 20% of the merger, high SFRs can persist after coalescence for almost a Gyr. Thus, although we should not have missed a large number of mergers due to partners falling off the inspection stamps, we may have graded a number of “just-merged” systems as non-mergers.

Fortunately, asymmetry metrics can be high during this period. Although a comparison of visual to quantitative metrics is not ideal, this suggests we should have captured many coalesced objects; highly-disturbed “isolated” systems would receive high merger grades. Hence, we believe the dominant source of identification uncertainty is likely to be the fraction of a merger over which prominent asymmetries are visible, which is about a third to half. In the maximal case, then, we could have underestimated the number of major-merging starbursts by a factor of ~ 3 .

However, while identification uncertainties may permit an SB merger-fraction high enough to account for the number of PSBs, uncertainties in the efficacy of such events in creating bulge-dominated, quiescent remnants appear to run in the opposite direction. First, *none* of the “Sbc” mergers from Lotz et al. (2008) terminate in non-starforming systems. Second, according to Hopkins et al. (2010, see their Fig. 15), assuming most of our disky SBs are indeed CSF-derived or fall into their “gas-rich” category, bulge formation is preferentially *suppressed* in mergers of these systems compared to those involving bulge-dominated and/or gas-poor galaxies. Combined, these effects might drastically reduce the number of major-merging SBs that could result in both bulge-dominated and quiescent remnants, i.e., systems which actually resemble our PSBs.

One could argue that the companion of a merging SB – which may not have been captured in the spectroscopic catalogue – might be bulge-dominated / gas-poor and therefore that the remnant would efficiently grow a bulge. However, mergers involving local red and blue galaxies – a proxy for this scenario – have been estimated by Chou et al. (2012) to be about an order of magnitude less common than mergers involving two blue galaxies. Therefore, though the analogy is not perfect, the probability that most of our SB mergers involve a gas-poor companion appears low.

Finally, there may be a more general constraint to consider. Both numerical (e.g., Lotz et al. 2008, 2010b) and observational studies (e.g., Poggianti et al. 1999) suggest that bulge-building (in mergers or otherwise) is delayed with respect to the cessation of starburst activity. If the delay is significant and a large portion of poststarbursts come from CSF-derived SBs (which are likely to be disk-dominated), then a substantial fraction of PSBs should be disky. This is clearly not the case (see Table 3).

In sum, mis-identification problems could perhaps provide a three-fold boost to the number of major-merging SBs, but it is likely that uncertainties in remnant properties and the effects of delayed morphological versus spectroscopic transformation (greatly) suppress this factor. So, although we cannot rule-out CSF-derived, major-

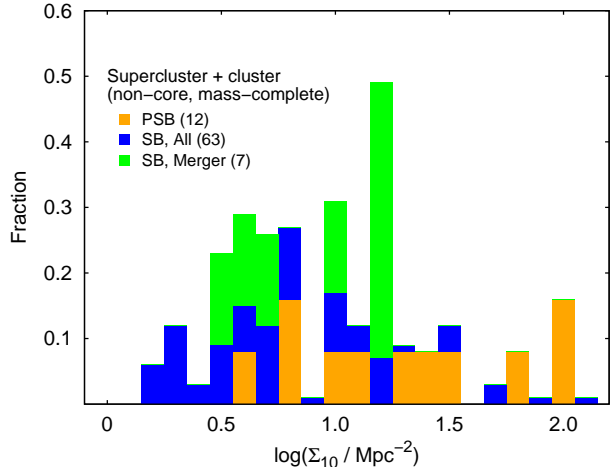


FIG. 7.— Surface densities (measured to the ten nearest-neighbors) of the environments of cluster PSB and SB systems. SBs plausibly involved in major-mergers (green histogram; see text Section 5.1) sample the underlying starburst population (blue histogram) in an unbiased fashion while PSBs (orange histograms) live preferentially in higher-density regions.

merging SBs as progenitors of a sizable fraction of our PSBs, it seems unlikely that they are responsible for most of this population given their baseline factor of 3 shortfall in numbers.

5.1. An Additional Constraint

There is one further piece of evidence we can offer that speaks against a CSF-derived, major-merger driven origin for most poststarbursts: the cluster galaxy correlation function. As shown in Paper II (see Figs. 4 & 6, therein) the active and poststarbursts (at least in clusters) have very different spatial distributions. Perhaps unsurprisingly, the SBs track CSFs, appearing relatively uniformly over the faces of our clusters, while the PSBs track the PASs, remaining centrally concentrated. (Recall the paucity of PSBs in the supercluster sample, above.) Therefore, even if we have somehow massively underestimated the number of mergers or all of our merging SBs are in fact on their way to becoming appropriately spheroidal / quiescent (neither of which do we think to be the case) they would still have to rearrange themselves spatially in order to account for all of the PSBs.

To test this, we relax our definition of “confirmed” major-mergers to include all (mass-complete) SBs with grades > 0 and compare the local environments of these galaxies versus those of the PSBs. (There are too few of these systems to adequately constrain their correlation function.) The results – using the surface density of a galaxy’s ten nearest-neighbors to parameterize “local environment” – are plotted in Figure 7.¹²

From these histograms, we can see that (plausibly) merging SBs do not preferentially live in denser regions than the rest of the starburst population while the PSBs clearly do. Indeed, approximately half of the latter systems are found at densities where there are no major-merging SBs (though still some non-merging SBs). A

¹²This analysis for field galaxies reveals no significant difference between the density distributions of any of our spectral types. This is likely because the spectroscopic catalogue samples the volume in this environment too sparsely to obtain a meaningful measurement.

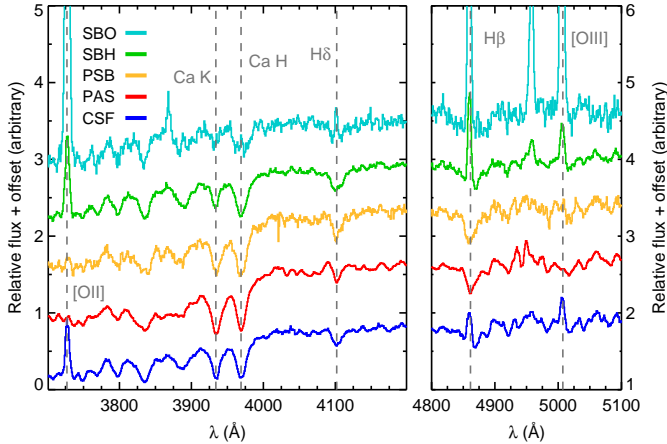


FIG. 8.— Mean composite spectra of the ICBS spectral types normalized to the CSF continuum surrounding $H\delta$ and [OIII]. Note that many SBHs – which comprise 77% of the SBs considered here – are *Spitzer-24* μm sources and [OII] emission may therefore be strongly extinguished. A considerable number of these systems may also be decaying starbursts (see Dressler et al. 2009, and Paper II). Although spectroscopically the SBH–PSB ties are strong – the former appearing as PSBs with emission – structurally they are quite divergent, suggesting evolutionary connections are weak.

larger sample is needed to draw definitive conclusions, but it seems from our data that many major-merging, CSF-derived SBs do not have the proper spatial distribution to be the progenitors of our poststarbursts, even if the aforementioned uncertainties in merger fractions, etc. might allow them to account for the total number of these systems. (Further, if this plot is representative of the true major-merging SB population, it could suggest that we have actually *overestimated* the number of candidate PSB progenitors by about a factor of two, since only half of merging SBs live in environments similar to the PSBs. This would further reduce the mis-identification enhancements discussed, above.)

It is of course possible that a conspiracy is at work, i.e., that PSBs reflect the most efficient bulge-forming mergers and we are missing those SBs which recently underwent a major-merger in the denser regions of our superclusters (at least). However, given the close resemblance of the poststarbursts to an existing population of appropriately bulge-dominated galaxies with an inherently similar spatial correlation function, a more straightforward interpretation of the data is that a large fraction of these galaxies are born from the passive population. If so, a non-starforming PAS–PSB–PAS recycling loop is almost certainly operating in parallel to the starforming loop described, above.

We should stress that, from a purely spectroscopic standpoint, this result is surprising. Figure 8 shows composite spectra of the ICBS spectral types. The resemblance between our SBs and PSBs (especially in the depth of $H\delta$, higher-order Balmer lines, and the relative strengths of Ca H and K) is apparent, here, with the latter appearing essentially as emission-less versions of the former. Hence, given only these data, the evolutionary scenario has great appeal! It is only when information is combined across multiple domains – photometric, spectroscopic, and morphological – that persuasive alternative interpretations emerge.

5.2. The Starburst Mechanism

While a range of plausible (if not operational) triggering mechanisms are consistent with the SB–CSF structural relationship (e.g., tidal disruptions, intrinsic disk instabilities, and simple gas accretion, as well as minor-mergers) minor-mergers appear to be the most likely candidate for producing those starbursts that lead to most PSBs. The reason is simply that passive galaxies lack large gaseous disks and are known to possess hot halos which would stifle cold-mode IGM accretion (Forman et al. 1985; Mulchaey & Jeltama 2010). Further, taking numbers from Lotz et al. (2011) and Newman et al. (2012), respectively, minor-merger rates of ~ 3 times the major-merger rate and close-companion fractions of $\sim 13 - 18\%$ are both the right size to allow these interactions to explain the $\sim 1:10$ PSB:PAS ratio we find. While we cannot definitively say what fraction of *all* SBs (CSF- and PAS-derived) are the result of minor-mergers, it is reasonable to suspect that these events occur in a similar fashion across PAS/CSF hosts (Woods & Geller 2007) suggesting that these interactions could be a significant-to-dominant source for intermediate-redshift starbursts.

5.3. Cluster Cores: an Aside

As noted in Section 1, the recycling scenario discussed above is expected to break down in cluster cores. Here, the SB:PSB ratio climbs to ~ 1 , and the PAS fraction rises rapidly at the expense of the CSFs, implying CSF \rightarrow PAS evolution is almost certainly active. This is not surprising: the dense ICM in these regions should prevent infalling SBs from rejoining the CSF population (breaking the starforming recycling loop) and – as has been known for decades – actively quench CSF galaxies through, e.g., ram-pressure stripping. While starbursts are thus only incidentally connected to PAS build-up – the global extinguishing of star formation affects the more numerous CSFs as well as the SBs – we do expect them to be the dominant source of core PSBs as no low-mass, gas-rich systems should survive long enough in these regions to accrete onto PASs.

Though projection effects and small sample size prohibit any definitive conclusions, the plot of cluster core Sérsic index distributions in the left panel of Fig. 5 suggests something consistent with this scenario is taking place. Here, the PSBs are seen to lose their high- n tail (as noted previously by the MORPHS collaboration, Dressler et al. 1999) and depart significantly from the PASs, falling squarely between these and the still-disk SBs. This is the signal we would expect if core SBs and PSBs reflect larger-radius accretions onto disk CSFs and their subsequent ICM-driven quenching. However, the similarity of core PSBs to core CSFs also suggests that some of these systems may be the results of ICM-triggered bursts (Bekki & Couch 2003) or the most extreme examples of post-truncation galaxies.

6. CONCLUSION

NIR structural measurements from > 1600 field and cluster galaxies ($0.31 < z < 0.54$) in the IMACS Cluster Building Survey support a cross-environmental scenario presented in Dressler et al. (2013) regarding the origin

and role of (post-)starburst galaxies and their connection to non-burst systems. We find:

- 1) little-to-no structural similarity between active and poststarburst systems outside of cluster cores. Modulo uncertainties about the contribution of major-mergers, this indicates that $\text{CSF} \rightarrow \text{SB} \rightarrow \text{PSB} \rightarrow \text{PAS}$ evolution is weak in almost all environments;
- 2) strong ties between SB–CSF and PSB–PAS classes, suggesting that most (post-)starbursts are transient “blips” in the lives of ordinary starforming and quiescent galaxies. Given the diskiness of the starforming systems, these relationships independently suggest that a gentle mechanism (likely minor-mergers) is responsible for the production of most intermediate-redshift starbursts;
- 3) evidence that, in cluster cores, this picture may

reverse, with environmentally specific agents providing a channel for $\text{CSF} \rightarrow \text{SB} \rightarrow \text{PSB} \rightarrow \text{PAS}$ evolution.

ACKNOWLEDGEMENTS

LA thanks Drs. Daniel Kelson and Chen Peng as well as Song Huang for generously sharing their time and insight. He also thanks Gabriel Prieto, Geraldo Valladares, and the rest of the LCO staff for their patience in supporting and skill in executing the observations analyzed here. AD and AO acknowledge the support of the NSF grant AST-0407343. All the authors thank NASA for its support through nasa-jpl 1310394. BV and BP acknowledge financial support from ASI contract I/016/07/0 and ASI-INAF I/009/10/0. MDG thanks the Research Corporation for support of this work through a Cottrell Scholars Award.

REFERENCES

- Bahe, Y. M., McCarthy, I. G., Balogh, M. L., & Font, A. S. 2012, ArXiv e-prints
- Balogh, M. L., Miller, C., Nichol, R., Zabludoff, A., & Goto, T. 2005, *MNRAS*, 360, 587
- Balogh, M. L., Navarro, J. F., & Morris, S. L. 2000, *ApJ*, 540, 113
- Barden, M., Häußler, B., Peng, C. Y., McIntosh, D. H., & Guo, Y. 2012, *MNRAS*, 422, 449
- Bekki, K., & Couch, W. J. 2003, *ApJ*, 596, L13
- Bekki, K., Couch, W. J., & Shioya, Y. 2002, *ApJ*, 577, 651
- Bell, E. F., Phleps, S., Somerville, R. S., et al. 2006, *ApJ*, 652, 270
- Bell, E. F., van der Wel, A., Papovich, C., et al. 2012, *ApJ*, 753, 167
- Benson, A. J., Džanović, D., Frenk, C. S., & Sharples, R. 2007, *MNRAS*, 379, 841
- Bertin, E. 2010a, *Astrophysics Source Code Library*, 10063
- , 2010b, *Astrophysics Source Code Library*, 10068
- Bertin, E., & Arnouts, S. 1996, *A&AS*, 117, 393
- Blanton, M. R., Schlegel, D. J., Strauss, M. A., et al. 2005, *AJ*, 129, 2562
- Butcher, H., & Oemler, Jr., A. 1978a, *ApJ*, 219, 18
- Chou, R. C. Y., Bridge, C. R., & Abraham, R. G. 2012, ArXiv e-prints
- Conselice, C. J. 2009, *MNRAS*, 399, L16
- Couch, W. J., & Sharples, R. M. 1987, *MNRAS*, 229, 423
- De Lucia, G., Poggianti, B. M., Aragón-Salamanca, A., et al. 2004, *ApJ*, 610, L77
- Dressler, A. 1980, *ApJ*, 236, 351
- Dressler, A., & Gunn, J. E. 1983, *ApJ*, 270, 7
- Dressler, A., Oemler, A., Gladders, M. G., et al. 2009, *ApJ*, 699, L130
- Dressler, A., Smail, I., Poggianti, B. M., et al. 1999, *ApJS*, 122, 51
- Dressler, A., Oemler, Jr., A., Couch, W. J., et al. 1997, *ApJ*, 490, 577
- Dressler, A., Bigelow, B., Hare, T., et al. 2011, *PASP*, 123, 288
- Faber, S. M., Willmer, C. N. A., Wolf, C., et al. 2007, *ApJ*, 665, 265
- Fakhouri, O., & Ma, C.-P. 2009, *MNRAS*, 394, 1825
- Fasano, G., Vanzella, E., Dressler, A., et al. 2012, *MNRAS*, 420, 926
- Fisher, D. B., & Drory, N. 2008, in *Astronomical Society of the Pacific Conference Series*, Vol. 396, *Formation and Evolution of Galaxy Disks*, ed. J. G. Funes & E. M. Corsini, 309
- Forman, W., Jones, C., & Tucker, W. 1985, *ApJ*, 293, 102
- Gao, L., Navarro, J. F., Frenk, C. S., et al. 2012, *MNRAS*, 425, 2169
- Gladders, M. D., & Yee, H. K. C. 2000, *AJ*, 120, 2148
- , 2005, *ApJS*, 157, 1
- Gunn, J. E., & Gott, III, J. R. 1972, *ApJ*, 176, 1
- Häussler, B., McIntosh, D. H., Barden, M., et al. 2007, *ApJS*, 172, 615
- Hogg, D. W., Masjedi, M., Berlind, A. A., et al. 2006, *ApJ*, 650, 763
- Hopkins, P. F., Croton, D., Bundy, K., et al. 2010, *ApJ*, 724, 915
- Hoyos, C., den Brok, M., Verdoes Kleijn, G., et al. 2011, *MNRAS*, 411, 2439
- Kauffmann, G. 1995, *MNRAS*, 274, 153
- Kaviraj, S., Peirani, S., Khochfar, S., Silk, J., & Kay, S. 2009, *MNRAS*, 394, 1713
- Larson, R. B., Tinsley, B. M., & Caldwell, C. N. 1980, *ApJ*, 237, 692
- Lemaux, B. C., Lubin, L. M., Shapley, A., et al. 2010, *ApJ*, 716, 970
- Lotz, J. M., Jonsson, P., Cox, T. J., et al. 2011, *ApJ*, 742, 103
- Lotz, J. M., Jonsson, P., Cox, T. J., & Primack, J. R. 2008, *MNRAS*, 391, 1137
- , 2010a, *MNRAS*, 404, 590
- , 2010b, *MNRAS*, 404, 575
- McBride, J., Fakhouri, O., & Ma, C.-P. 2009, *MNRAS*, 398, 1858
- Mendel, J. T., Simard, L., Ellison, S. L., & Patton, D. R. 2012, ArXiv e-prints
- Mihos, J. C., & Hernquist, L. 1994, *ApJ*, 425, L13
- Moore, B., Diemand, J., & Stadel, J. 2004, in *IAU Colloq. 195: Outskirts of Galaxy Clusters: Intense Life in the Suburbs*, ed. A. Diaferio, 513–518
- Moran, S. M., Ellis, R. S., Treu, T., et al. 2007, *ApJ*, 671, 1503
- Moustakas, J., Coil, A., Aird, J., et al. 2013, ArXiv e-prints
- Mulchaey, J. S., & Jeltama, T. E. 2010, *ApJ*, 715, L1
- Newman, A. B., Ellis, R. S., Bundy, K., & Treu, T. 2012, *ApJ*, 746, 162
- Oemler, Jr., A., Dressler, A., Kelson, D., et al. 2009, *ApJ*, 693, 152
- Peng, C. Y., Ho, L. C., Impey, C. D., & Rix, H.-W. 2002, *AJ*, 124, 266
- Peng, C. Y., Ho, L. C., Impey, C. D., & Rix, H. W. 2007, in *Bulletin of the American Astronomical Society*, Vol. 39, *American Astronomical Society Meeting Abstracts*, 804
- Persson, S. E., Barkhouser, R., Birk, C., et al. 2008, in *Society of Photo-Optical Instrumentation Engineers (SPIE) Conference Series*, Vol. 7014, *Society of Photo-Optical Instrumentation Engineers (SPIE) Conference Series*
- Poggianti, B. M., Smail, I., Dressler, A., et al. 1999, *ApJ*, 518, 576
- Poggianti, B. M., Aragón-Salamanca, A., Zaritsky, D., et al. 2009, *ApJ*, 693, 112
- Postman, M., Franx, M., Cross, N. J. G., et al. 2005, *ApJ*, 623, 721
- Quintero, A. D., Hogg, D. W., Blanton, M. R., et al. 2004, *ApJ*, 602, 190
- Renzini, A. 2006, *ARA&A*, 44, 141
- Sérsic, J. L. 1968, *Atlas de galaxies australes*

- Tran, K.-V. H., Franx, M., Illingworth, G., Kelson, D. D., & van Dokkum, P. 2003, *ApJ*, 599, 865
- Tran, K.-V. H., Franx, M., Illingworth, G. D., et al. 2004, *ApJ*, 609, 683
- van der Wel, A. 2008, *ApJ*, 675, L13
- van der Wel, A., Holden, B. P., Franx, M., et al. 2007, *ApJ*, 670, 206
- Williams, R. J., Quadri, R. F., & Franx, M. 2011, *The Astrophysical Journal Letters*, 738, L25
- Woods, D. F., & Geller, M. J. 2007, *AJ*, 134, 527
- Yan, R., Newman, J. A., Faber, S. M., et al. 2009, *MNRAS*, 398, 735
- Yang, X., Mo, H. J., van den Bosch, F. C., et al. 2007, *ApJ*, 671, 153
- Yang, Y., Zabludoff, A. I., Zaritsky, D., & Mihos, J. C. 2008, *ApJ*, 688, 945
- Yoon, I., Weinberg, M. D., & Katz, N. 2011, *MNRAS*, 414, 1625
- York, D. G., Adelman, J., Anderson, Jr., J. E., et al. 2000, *AJ*, 120, 1579
- Zabludoff, A. I., Zaritsky, D., Lin, H., et al. 1996, *ApJ*, 466, 104